Hindawi
Journal of Advanced Transportation
Volume 2024, Article ID 8999086, 13 pages
https://doi.org/10.1155/2024/8999086

Research Article

Edge AI-Based Smart Intersection and Its Application for Traffic Signal Coordination: A Case Study in Pyeongtaek City, South Korea

Seongjin Lee,[1] Seungeon Baek,[1] Wang-Hee Woo,[2] Chiwon Ahn,[3] and Jinwon Yoon [1]

[1]*Nota AI Inc., Team ITS, 332 Teheran-ro, Gangnam-gu, Seoul 06212, Republic of Korea*
[2]*Pyeongtaek Urban Corporation, Department of Transportation Policy, 25, Doilyutong-gil, Pyeongtaek 17725, Gyeonggi, Republic of Korea*
[3]*University of Seoul, Department of Transportation Engineering, 163 Seoulsiripdaero, Dongdaemun-gu, Seoul 02504, Republic of Korea*

Correspondence should be addressed to Jinwon Yoon; jinwon.yoon@kaist.ac.kr

Received 25 November 2023; Revised 21 February 2024; Accepted 22 March 2024; Published 3 April 2024

Academic Editor: Seongjin Choi

Recently, smart intersections have emerged as a novel intelligent transportation system (ITS) solution that integrates traffic monitoring, optimal signal control, and even traffic safety. Although smart intersections have been prevalent in many cities, there are a few drawbacks in their practical operations. First, there are inevitable delays in transmitting and processing the video data. Second, there is still a need to develop a real-time signal control method leveraging the acquired data from smart intersections. Thus, this study aims to construct edge AI-based smart intersections and to provide their application for traffic signal coordination. To this end, we install smart intersections on three consecutive intersections of Route 45 in Pyeongtaek city, South Korea. The real-time traffic data are collected by an edge AI video analysis model which is compressed and optimized for its operation in on-site edge devices. The optimized model maintains a similar level of accuracy (93.64%), even if the size is reduced by 97.8% compared to the original. Next, we utilize the LT2 model to treat the coordination failure problem in nonpeak hours occurring unnecessary delays of the side-streets with relatively high demands. We complement some constraint conditions in order to consider the compatibility with the current legacy system. The experiment is conducted on a virtual environment of which geometry and traffic demand are configured based on the features of the study site. The numerical results conclude that the optimal offsets calculated by the LT2 model effectively manage bandwidths for multidirectional flows based on the real-time traffic demands collected from the edge AI-based smart intersections. This study contributes to serve high-resolution real-time traffic data using edge AI on smart intersections and to provide a case study for signal coordination.

1. Introduction

As the social costs of traffic congestion steadily increase, there has been a growing interest in optimizing the traffic signal controls in urban areas. The adaptive control [1–3] is the one of the most well-known methods for optimizing the signal controls on road networks; however, it has the limitations in practical use regarding the stability of data collection and the feasibility of real-time computation [4]. For this reason, many cities still operate pretimed control of which signal timings are calculated based on the annual average daily traffic (AADT) statistics. Accordingly, an alternative called "Smart Intersections" has been introduced recently [5, 6], which is a new intelligent transportation system (ITS) solution integrating the traffic monitoring, optimal signal control, and even traffic safety. Smart intersections apply the artificial intelligence (AI) technique to analyze video data collected from the traffic monitoring closed-circuit televisions (CCTVs) and extract the useful traffic data and utilize the processed data for traffic signal optimizations and pedestrian safety controls, etc.

There are several advantages of smart intersections, as they make use of CCTV video data. First of all, smart intersections are cost-effective since they do not require the road works for the construction or maintenance, unlike the ground-embedded loop detectors. Moreover, unlike other conventional traffic sensors, smart intersections can provide both point- and section-based information. In addition, smart intersections are expected to have a great potential for the signal control optimization because they can provide the contextual information, such as vehicle type classification, queue length, or turning ratio.

Ideally, smart intersection is an all-in-one solution for real-time intersection management that integrates multiple functions for traffic monitoring and control. However, there is a critical drawback regarding the data transmission and processing. In the current ITS system, the collected CCTV video data are practically transmitted to the ITS center and processed in a high-performance computer. This is because it is too heavy to operate the AI video analysis model on the on-site equipment, such as roadside unit (RSU). Accordingly, it inevitably causes at least a few seconds or minutes delays. Another issue regards their application for signal controls. Even if smart intersections have enabled to acquire more abundant traffic data, there are few cases leveraging smart intersection data. Recently, several data-driven signal control methods based on AI have been proposed [7–9]; however, these techniques are not matured to be practically implemented yet. Moreover, many of these initiatives require the establishment of extra equipment for collecting additional data, or some are not compatible with existing legacy signal control systems.

Thus, our goal is to construct edge AI-based smart intersections utilizing AI optimization techniques and to provide their application for traffic signal coordination. To this end, we first install smart intersections (see Figure 1) on three consecutive intersections of Route 45 in Pyeongtaek city. Then, the video images collected from CCTVs are analyzed on the edge devices by applying the edge AI video analysis model to extract the meaningful traffic data in real time. For the edge AI model, we compress the AI video analysis model into a small-sized one and optimize it to be well operated in the on-site edge device. Next, we provide a case study of traffic signal coordination as an application of the installed smart intersections. The purpose of this case study is to verify the effectiveness of smart intersections on signal controls before their implementation on real roads. Thus, the experiment is conducted on a simulated environment configured identically to the study site. Moreover, we complement some constraint conditions on signal timing variables in order to consider the compatibility with the current legacy signal control system. The rest of the paper is constructed as follows. In the following section, the backgrounds of this research are provided. Then, the details for constructing smart intersections and the methodology are shown. Finally, the conclusion is proposed with the experimental results.

2. Related Works

2.1. Smart Intersections. Smart intersections are newly proposed ITS solutions in recent years which aim to optimize traffic monitoring and control by applying AI techniques. At first, smart intersections collect real-time traffic information by analyzing videos from traffic monitoring CCTVs with the computer vision (CV) methods. They detect specific objects in the image (detection), classify the detected objects into several classes (classification), and track the movements of the objects (tracking). Starting with the first application of applying deep learning to the image processing in 2012 [10], the video analysis has been greatly matured with the improvement of deep learning techniques.

The initial algorithms for the video analysis are basically based on the convolutional neural networks (CNNs). CNNs are specialized for detecting specific features of the image, and they are still frequently used in the field of image processing. Starting with Regions with CNN features (R-CNN) [11], which search only specific areas of an image, algorithms such as Fast R-CNN [12] and Faster R-CNN [13] were proposed to improve the efficiency for the computational; however, these methods still have limitation in real-time video processing. In 2016, a new algorithm called you only look once (YOLO) [14] can achieve high accuracy with minimal computation, enabling object detection and classification simultaneously. Furthermore, recently developed YOLO v8 (by Ultralytics in Jan. 2023) and single shot multibox detector (SSD) [15] have highly improved the video analysis techniques for smart intersections.

When it comes to the traffic data, smart intersections have several advantages over traditional sensor-based traffic data collection. Most of all, smart intersections can provide both the point- and the section-based information. For the point-based information, like the loop detector and laser scanner, smart intersections can provide the flow information for vehicles and pedestrians by setting up a virtual line in the field of view (FoV) and counting the number of objects that cross the line. For the section-based information, for example, they can measure the queue length by recognizing the stopping vehicles in FoV, like radar and lidar. However, smart intersections, in particular, can estimate the space-mean speed by measuring travel times of the traversing vehicles since smart intersections can recognize the contextualized information. For example, they can classify the types of objects into normal vehicle, bus, truck, motorcycle, pedestrian, and even emergency vehicle and personal mobility (PM), unlike radar or lidar. Finally, smart intersections can provide individual vehicle's trajectories within FoV, which is the most powerful feature. Accordingly, for example, they can measure the turning ratios without installing additional road sensors.

However, there is a critical limitation on the current smart intersection system. As heavy-sized AI video analysis models cannot be operated in the on-site equipment, the current system transmits the obtained video to a high-performance server in ITS center, which causes at least a few seconds/minutes delays (approximately 1,000~7,000 ms at least in practice) (see Figure 2). Moreover, the existing system cannot be operated when the communication network is disconnected or where the network is not installed. To overcome this limitation, the potential use of edge AI (or called lightweight AI or on-device AI) techniques have newly been considered. It is expected that edge AI-based

Figure 1: Layout of the study site.

smart intersections enable to operate the lightweighted AI model within on-site equipment (edge device) and process the collected video data in real time. Besides, as the edge system only transmits processed message data (text data) rather than full-size video, it can reduce the cost of network communication and comply with the general data protection regulation (GDPR). Moreover, it saves storing cost since it is not necessary to store all the raw video data.

2.2. Traffic Signal Coordination. The signal coordination usually refers to the problem that controls the offsets of the intersection in a corridor to maximize the progression of the traffic flow for the mainstream. In general, the coordination methods aim to maximize the bandwidth which is the range of time in which a vehicle entering an upstream intersection can pass through a downstream intersection without stopping.

MAXBAND [16] is the first study which proposes the bandwidth maximization as for the signal coordination. In this study, the optimal offset values are calculated by mixed integer linear programming (MILP) to maximize the two-way progression along the corridor. On the other hand, MULTIBAND [17] complements the relaxation condition on the feasible region of the solution to overcome the limitation of MAXBAND in which the bandwidths for each intersection are symmetrically constant. It contributes to optimize the signal coordination by considering the capacity and traffic volume of individual intersection. In addition, AM-BAND [18] suggests the asymmetric bandwidth by relaxing the existing constraints that the bandwidth is determined symmetrically from the baseline.

Unlike the conventional methodologies that the bandwidth has been determined centered at the mainstream of the corridor, recent studies consider the turning flows from the minor stream as well. In particular, the LT2 model [19] maximizes the bandwidth for both the mainstream and the side-street left-turning traffic flows to mitigate the congestion of the side-street which is hardly considered in conventional methodologies. In addition, LT2 provides a detailed modeling for the queue clearance time at the downstream intersection by considering the traffic volume and signal control variables for the upstream intersection. Nonetheless, similar to the previous methods, LT2 also assumes the uniform distribution for the traffic generation based on statistical traffic volume aggregated in a large range of time window, which may not be appropriate to the actual traffic.

3. Problem Statement

3.1. Study Site. For the case study, we target the problem of traffic signal coordination in Route 45 of Pyeongtaek city, South Korea. We construct smart intersections in this target study area aiming to improve the signal coordination. Specifically, the spatial range includes three consecutive intersections of Route 45 in Pyeongtaek city, South Korea, as shown in Figure 1. This section is a major intercity arterial that connects the central Pyeongtaek area (North) to Asan city (South). This section also has a number of traffic demands not only for the commuting vehicles but also for the heavy vehicles, such as cargo trucks. As the majority of traffic demands travels from north to south, the signal coordination is set to accord with the same direction. However, this coordination setting is not effective to the nonpeak hour traffic demands since it yields unnecessary delays to the opposite direction (South ⟶ North) or turning flows. Thus, the temporal range of this study is configured as 13:00~16:00 when public petitions are frequently registered.

3.2. Current Status and Gaps. We first collect 24-hour traffic data on 18 May 2022 (Wednesday) after installing smart intersections to identify the current status and to investigate research gaps. The analyzed results are shown in Figure 3. The top of Figure 3 shows the changes in traffic volumes, while the bottom shows the turning flows during the time for TOD PLAN #2 (08:30~16:00) which includes the target temporal range (13:00~16:00). The results show that the study site has a high level of traffic demands during the peak hours, and the demand of the mainstream (North ⟶ South) is especially high. In addition, the majority of traffic demands at Pyeonggung-samgeori (3-way intersection in the middle) travel along with the mainstream; however, 11% merges to the opposite direction of the mainstream from the minor roads (Anjeong-ro).

The signal control for this study site is operated by pretimed TOD calculated based on AADT, and the signal information including phase design and minimum green time is shown in (Table 1). The overall TOD plans are given in Table 2. It is seen that each intersection has four TOD plans and shares the common schedule and cycle time since all the intersections belong to one subarea (SA). The time-space diagram for TOD PLAN #2 is plotted in ((a)), and it can be seen that the signal coordination is set to accord with the direction for the mainstream (North ⟶ South). Accordingly, the

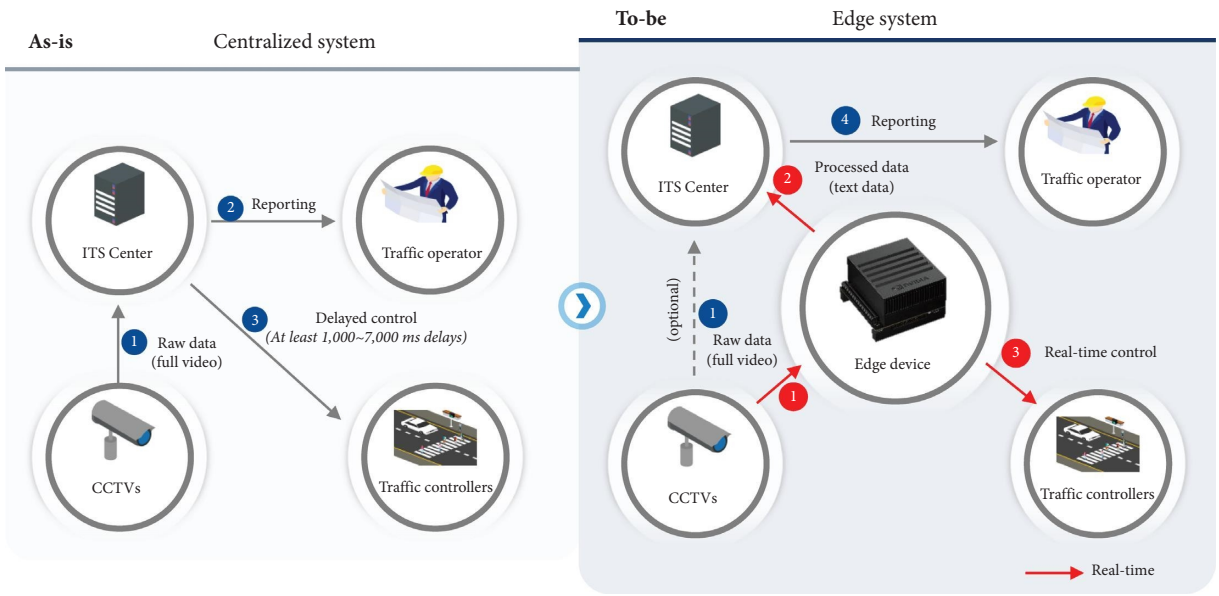

Figure 2: Comparison of smart intersections system.

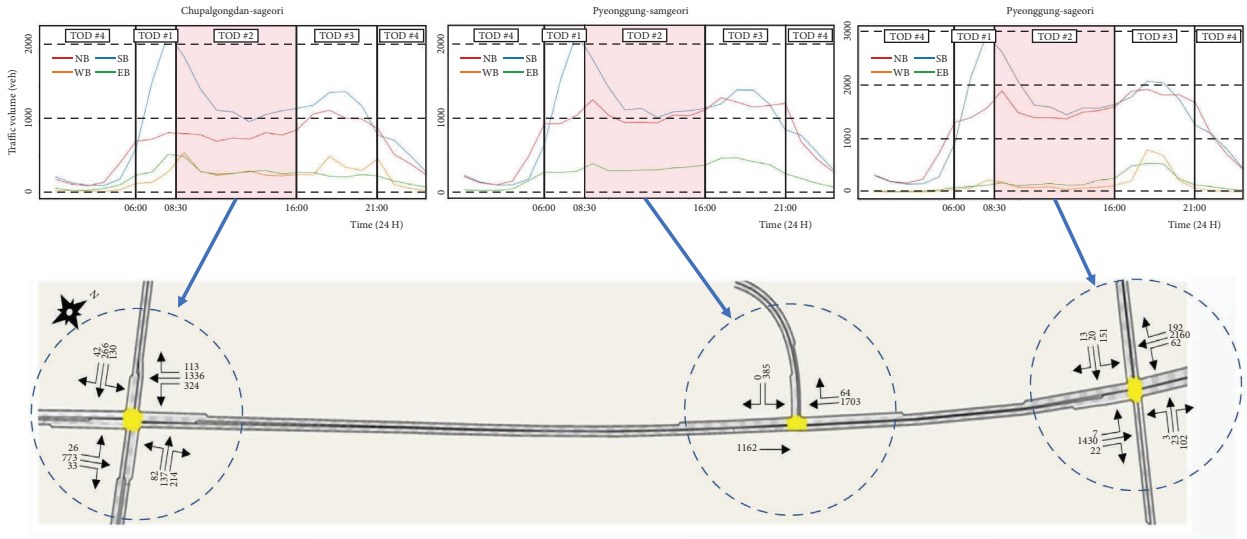

Figure 3: Traffic status of study site.

majority of the mainstream flows can pass through the area without stopping.

However, this coordination setting is not effective to the nonpeak hour traffic demands since the TOD plan is based on the aggregated statistical historical traffic data. For example, although the number of traffic flow for the opposite direction (Path 2 in Figure 4) increases up to 70% of that of the mainstream during the target time range 13:00~16:00, it fails to coordinate and the platoon is cut off at Pyeonggung-samgeori. In addition, the left-turning flow at Pyeonggung-samgeori merging into the opposite direction of the mainstream (Path 4 in Figure 4) increases up to 35% of that of the mainstream; however, the majority fails to coordinate, and the platoon is cut off at Pyeonggung-sageori (4-way intersection at north). In the meantime, even if the left-turning flow from the eastern approach of the Pyeonggung-sageori (Path 5 in Figure 4) decreases below 1% of that of the mainstream, it unnecessarily coordinates the signal so that the corresponding traffic flow can pass through the area without stopping. In conclusion, the existing signal coordination is only centered at the mainstream that results in coordination failure for the opposite direction and left-turning traffic demands in spite of their demand levels are not low.

4. Methodology

4.1. Construction of Edge AI-Based Smart Intersections. A key clue for resolving the coordination failure of the study site is to acquire real-time traffic flow information for each

Table 1: Signal phases (upward arrow points to north).

Intersection		Ø1	Ø2	Ø3	Ø4	Ø5
Chupalgongdan-sageori	Phase					
	Min. green	30	11	25	25	14
Pyeonggung-samgeori	Phase				—	—
	Min. green	34	25	8	—	—
Pyeonggung-sageori	Phase					—
	Min. green	28	14	17	27	—

Table 2: TOD plans.

Intersection		TOD	Cycle	Offset	∅1	∅2	∅3	∅4	∅5
Chupalgongdan-sageori	#1	06:00–08:30	200	9	45	14	27	25	89
	#2	08:30–16:00	150	12	51	20	27	25	27
	#3	16:00–21:00	180	147	61	40	27	25	27
	#4	21:00–06:00	150	135	51	20	27	25	27
Pyeonggung-samgeori	#1	06:00–08:30	200	45	150	35	15	—	—
	#2	08:30–16:00	150	62	100	35	15	—	—
	#3	16:00–21:00	180	6	130	35	15	—	—
	#4	21:00–06:00	150	44	106	29	15	—	—
Pyeonggung-sageori	#1	06:00–08:30	200	26	129	18	26	27	—
	#2	08:30–16:00	150	43	80	21	22	27	—
	#3	16:00–21:00	180	10	104	18	31	27	—
	#4	21:00–06:00	150	44	82	21	20	27	—

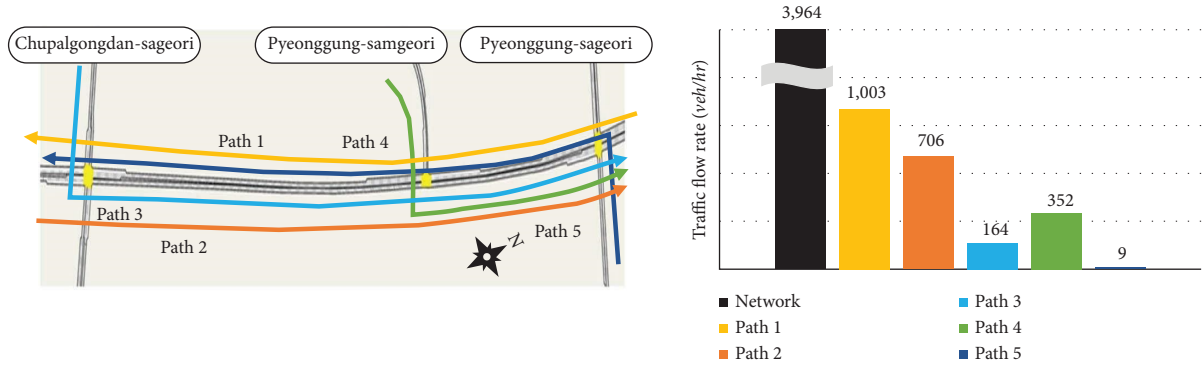

Figure 4: Subpaths for evaluation.

approaching link and recalculate offsets according to these data. Hence, we install CCTV cameras on the downstream of each approaching link to capture the turning flows and queue information. Additionally, we install edge devices on each intersection to process the collected video images from the CCTV cameras using the AI video analysis model in real time. The components are described as in (Figure 5).

Next, we have the optimized lightweight AI video analysis model via *NetsPresso* (AI optimization solution provided by Nota AI Inc. (https://netspresso.ai/)) (AI optimization platform developed by Nota Inc.). The mechanism of *NetsPresso* is as follows: at first, we have a pretrained object detection model using labeled intersection image data. In this study, we use YOLOX as a backbone which is a high-performance one-stage model employing a decoupled head [20], and the model is fine-tuned for each camera's FoV. Then, the importance for each filter of the CNN is measured using the structured pruning technique [21]. The importance is defined by the L^2-norm for the weight parameters of the CNN filter. The less important filters are removed to compress the model size. This process is repeated until the model size is smaller than the target size. Besides, for object tracking, we use the discriminative correlation filter (CDF)-based visual tracker [22]. Finally, the compressed model is converted and packaged to be mounted on the edge devices installed in the study site [20, 22]. (The specification of the edge device is shown in Table 3).

The region of interest (RoI) for the object detection is set as in Figure 6. At first, the range is set to be the maximum distance in the camera's FoV where the object's type is distinguishable, and the region is divided by each lane. Then, unlike the existing approaches for smart intersections, we additionally include the part of the upstream of opposite direction in the RoI to measure both inflows and outflows. Figure 6(b) shows the result of inference of the AI model, and it can be seen that the objects in both downstream and upstream are detected and classified into each vehicle type.

From the video analysis, we collect the traffic data: traffic volume and the number of queueing vehicles by lane and by vehicle type, average speed of each lane (space-mean speed in each RoI). At first, the objects are classified into three categories: car, bus, and truck. Then, the traffic volume is measured by setting up a virtual line and counting the number of vehicles crossing the line. The queue information is measured by counting the number of vehicles moving at less than 5 km/h for a certain period. Furthermore, the travel time of each vehicle passing through the RoI range is measured, and the space-mean speed for the RoI is estimated by harmonically averaging the travel time.

4.2. Traffic Signal Coordination Method. As this study aims to treat the signal coordination failure problem in nonpeak hours occurring unnecessary delays of the side-streets with relatively high demands, we propose to utilize the LT2 model

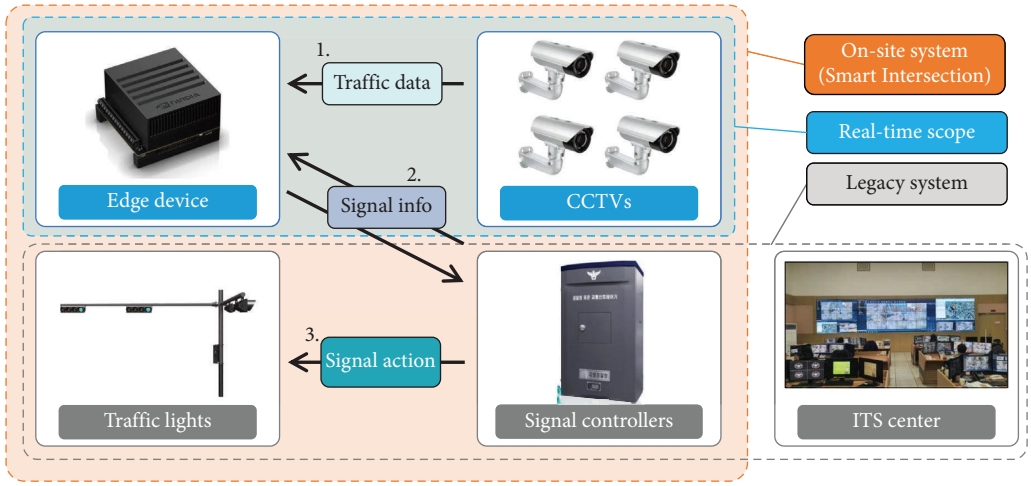

Figure 5: Components of smart intersection.

Table 3: Specification of edge device.

Product	Item	Detail
NVIDIA Jetson AGX Xavier	CPU	ARMv8 processor rev 0(v8l)
	GPU	512-core volta GPU with tensor cores
	RAM	32 GB
	Storage	32 GB
	OS	Ubuntu 18.04.5 LTS (kernel: 4.9.140)
	NIC	RJ45 1 port
	S/W	Python 3.6.9
		CUDA 10.2.89

(a) (b)

Figure 6: Result of object detection of smart intersection. (a) Region of interest (RoI) setting. (b) AI model inference for object detection.

to coordinate the multidirectional traffic flows. We adopt the basic structure of the LT2 model as the backbone; however, we partially adjust the model to use the real-time traffic data collected from the smart intersection. Besides, we derive the conditions for its application in the legacy signal control system and add them into the constraints.

First, the traffic volumes of each lane collected from the smart intersection are aggregated according to the turning directions. Then, the aggregated directional flows are used as a major input variable for the model. Second, we adopt the objective function which is the jointly maximization of the bidirectional bandwidths and the side-street left-turning bandwidths, as in equation (1):

$$\text{Maximize} \sum_{i=1}^{n-1} \left(\text{at}_i \times \text{bt}_i + \overline{\text{at}}_i \times \overline{\text{bt}}_i + \text{al}_i \times \text{bl}_i + \overline{\text{al}}_i \times \overline{\text{bl}}_i \right), \quad (1)$$

where $\text{at}_i = v_i^{\text{mt}}/S_i$, $\text{al}_i = v_i^{\text{sl}}/S_i$, $\overline{\text{at}}_i = \overline{v}_{i+1}^{\text{mt}}/\overline{S}_i$, $\overline{\text{al}}_i = \overline{v}_{i+1}^{\text{sl}}/\overline{S}_i$, $i = 1, 2, \ldots, n-1$. The key constraint conditions of LT2 are as follows (directly referred from [19]): for $i = 1, 2, \ldots, n-1$,

$$t_i + \overline{t}_i + (w_i - w_{i+1}) + (\overline{w}_{i+1} - \overline{w}_i) + \Delta_i - \Delta_{i+1} = \left(-\frac{1}{2}\right)(r_i + \overline{r}_{i+1}) + \left(\frac{1}{2}\right)(\overline{r}_i + r_{i+1}) + (\overline{\tau}_i + \tau_{i+1}) + m_i \tag{2}$$

$$\tau_{i+1} \geq \begin{cases} (r_i + t_i - \mathrm{dc}_i) \cdot q^{\mathrm{sr}}_{i,i+1} \cdot \mathrm{qd}_i, & \mathrm{dls}_i + \mathrm{Ls}_i + t_i \leq \mathrm{dc}_i \\ \left((\mathrm{dls}_i + \mathrm{Ls}_i + t_i - \mathrm{dc}_i) \cdot q^{\mathrm{sl}}_{i,i+1} + (r_i + t_i - \mathrm{dc}_i) \cdot q^{\mathrm{sr}}_{i,i+1}\right) \cdot \mathrm{qd}_{i+1}, & \mathrm{dls}_i < \mathrm{dc}_i - t_i \leq \mathrm{dls}_i + \mathrm{Ls}_i \\ \left(\mathrm{Ls}_i \cdot q^{\mathrm{sl}}_{i,i+1} + (r_i + t_i - \mathrm{dc}_i) \cdot q^{sr}_{i,i+1}\right) \cdot \mathrm{qd}_{i+1}, & 0 < \mathrm{dc}_i - t_i \leq \mathrm{dls}_i \\ \dfrac{\left((t_i - \mathrm{dc}_i) \cdot q^{\mathrm{mt}}_{i,i+1} + \mathrm{Ls}_i \cdot q^{\mathrm{sl}}_{i,i+1} + r_i \cdot q^{\mathrm{sr}}_{i,i+1}\right)}{\mathrm{qd}_{i+1}}, & \mathrm{dc}_i \leq t_i, \end{cases} \tag{3}$$

$$\mathrm{bl}_i = \begin{cases} \mathrm{Ls}_i, & \mathrm{dls}_i + \mathrm{Ls}_i + t_i - \mathrm{dc}_i \leq 0 \\ \mathrm{dc}_i - t_i - \mathrm{dls}_i, & 0 < \mathrm{dls}_i + \mathrm{Ls}_i + t_i - \mathrm{dc}_i \leq \mathrm{Ls}_i, \\ 0, & \mathrm{Ls}_i < \mathrm{dls}_i + \mathrm{Ls}_i + t_i - \mathrm{dc}_i \leq r_{i+1} \\ \mathrm{dls}_i + \mathrm{Ls}_i + t_i - \mathrm{dc}_i - r_{i+1}, & r_{i+1} < \mathrm{dls}_i + \mathrm{Ls}_i + t_i - \mathrm{dc}_i \leq r_{i+1} + \mathrm{Ls}_i \\ \mathrm{Ls}_i, & r_{i+1} + \mathrm{Ls}_i < \mathrm{dls}_i + \mathrm{Ls}_i + t_i - \mathrm{dc}_i. \end{cases} \tag{4}$$

Equation (2) is to utilize the constraints of MULTIBAND, which is fundamentally required to achieve an equation coordinated bandwidth model. Equation (3) is to relax the existing constraints on the bandwidth by modeling the queue clearance time with observed upstream inflows. Equation (4) is to describe the relationship between the bandwidth of side-street turning flow and the signal phases.

Third, we additionally consider the following constraint conditions regarding the legacy signal control system: preservation of cycle time and preservation of green split in each TOD. In the current legacy system of South Korea, changing cycle time only for a few intersections in one SA group is not allowed. Likewise, changes of green splits are not easy to be allowed due to the stability issue so that we set it as a hard constraint. Instead, simply changing the offset values is relatively easy to be applied in the legacy system, as it only changes the starting time of the existing TOD plans. Other crucial constraints, such as preservation of phase design, phase sequence, ring design, are also considered.

Finally, we interpret the output of the LT2 model as the offset values of each intersection, as the bandwidth which is the output of LT2 model can be simplified to an equation by the offsets according to the above constraints. The description for other variables is summarized in Table 4.

5. Experiments

5.1. Experimental Design. We set up a virtual environment using AIMSUN, a microscopic traffic simulation tool to evaluate the performance of the proposed model in the target area. To replicate the installed smart intersections, the arterial links are divided into upstream, midstream, and downstream sections based on the RoI range of the camera. The upstream and downstream sections represent the areas within the RoI where the traffic data can be extracted, and the midstream is a blind section so that the traffic data in this section are not collected.

Next, the collected real-time traffic data are aggregated at intervals identical to the signal cycle length, constituting one data unit. Traffic variables, such as in/outflow and turning ratios, are derived within the unit. Then, the outflow and inflow are embedded into the downstream and upstream links, and the turning ratios are embedded into each node. This approach allows to create a virtual traffic environment that is similar to the actual study site. To relieve the data fluctuation, these units are aggregated in 15 minutes and it configures the demand scenario. The model performances are evaluated in the scenarios with the same random seed, and the final result is derived by averaging the results across the scenarios of 10 different random seeds.

To measure the effects of the proposed model, we compare the performance with other well-known signal coordination methods, such as MULTIBAND, PASSER2, and the existing TOD plan. For a fair comparison, we maintain the same constraint conditions as the legacy system, such as cycle length, phase order, and green splits, but it only controls the offsets. Additionally, this approach enables to solely evaluate the impact of changes in the bandwidth to the traffic flows, excluding other factors.

For the evaluation, we employ the average number of stops as the primary measure of effectiveness (MoE) since this study aims to maximize the bandwidth of bidirectional and turning traffic flows through offset control. In addition, the average travel time and the average delay serve as secondary evaluation metrics to measure the network performance. The average number of stops is normalized by the travel distance to obtain the average number of stops per unit length (#/km) since each vehicle has a different route.

Table 4: Key model parameters and description.

Notation	Description
at_i ($\overline{at}_i$)	Weight for out/in-bound arterial progression through band on section i
bt_i ($\overline{bt}_i$)	Out/in-bound arterial progression through bandwidth (cycles) on section i
al_i ($\overline{al}_i$)	Weight for out/in-bound progression cross band on section i
bl_i ($\overline{bl}_i$)	Out/in-bound side-street left turn green bandwidth (cycles) on section i
v_i^{mt} ($\overline{v}_i^{mt}$)	Out/in-bound arterial through volume (veh/hr) at S_i
v_i^{sl} ($\overline{v}_i^{sl}$)	Out/in-bound side-street left-turn volume (veh/hr) at S_i
S_i ($\overline{S}_i$)	Saturation flow on section i
r_i ($\overline{r}_i$)	Out/in-bound red time at S_i (cycles)
w_i ($\overline{w}_i$)	Time from right side of red at S_i to S_{i+1} outbound (S_{i+1} to S_i inbound) (cycles)
t_i ($\overline{t}_i$)	Travel time from S_i to S_{i+1} outbound (S_{i+1} to S_i inbound) (cycles)
$\varnothing_i$ ($\overline{\varnothing}_i$)	Time from center of an out/in-bound red at S_i to the center of a particular out/in-bound red at S_{i+1}
Δ_i	Time from center of $\overline{r}_i$ to nearest center of r_i (cycles)
τ_i ($\overline{\tau}_i$)	Outbound (inbound) queue clearance time at S_i (cycles)
m_i	Loop integer
Ls_i ($\overline{Ls}_i$)	Out/in-bound left-turn green time on cross street at S_i (cycles)
dls_i ($\overline{dls}_i$)	Time from end of out/in-bound arterial through green phase to start of out/in-bound side-street left turn green phase at S_i (cycles)
$q_{i,i+1}^{mt}$ ($\overline{q}_{i,i+1}^{mt}$)	Uniform arrival rate (veh/sec) for vehicles departing during arterial through green from S_i to S_{i+1} outbound (S_{i+1} to S_i inbound)
$q_{i,i+1}^{sl}$ ($\overline{q}_{i,i+1}^{sl}$)	Uniform arrival rate (veh/sec) for vehicles departing during side-street left-turn green from S_i to S_{i+1} outbound (S_{i+1} to S_i inbound)
$q_{i,i+1}^{sr}$ ($\overline{q}_{i,i+1}^{sr}$)	Uniform arrival rate (veh/sec) for vehicles turning right from cross street during red time of coordinated phase from S_i to S_{i+1} outbound (S_{i+1} to S_i inbound)
dc_i ($\overline{dc}_i$)	Outin-bound time difference of red starts of coordinated phase between S_i (S_{i+1}) and S_{i+1} (S_i) (cycles)
qd_i ($\overline{qd}_i$)	Out/in-bound arterial saturation through flow headway (sec/veh) at S_i

Similarly, the other two time-related metrics are also normalized as the average travel time per unit travel distance (sec/km) and the average delay per unit travel distance (sec/km), respectively.

The explicit forms of these metrics are as follows: for all vehicles entering the network, veh_i $(i = 1, 2, \ldots, N)$, the vehicles that traverse each route P_j are denoted by $P_j = \left\{\text{veh}_{j_1}, \text{veh}_{j_2}, \ldots, \text{veh}_{j_{N(j)}}\right\}$, and the travel distance of P_j is denoted by $L(j)$. Subsequently, the average number of stops throughout the network and the average number of stops for each P_j are denoted by $\overline{s}$ and $\overline{s}_j$, respectively, and they can be calculated based on the stop time of each vehicle i, denoted by $s(i)$.

$$\overline{s} = \frac{\sum_i s(i)}{N \cdot \sum_j L(j)}, \overline{s}_j = \frac{\sum_k s(j_k)}{N(j) \cdot L(j)} \tag{5}$$

Similarly, if we denote the travel time of i by $t(i)$ and the delay time by $d(i)$, then the overall average travel time in the network $\overline{t}$, average delay $\overline{d}$, the average travel time $\overline{t}_j$, and the average delay $\overline{d}_j$ for each route P_j are calculated by

$$\begin{aligned} \overline{t} &= \frac{\sum_i t(i)}{N \cdot \sum_j L(j)}, \overline{d} = \frac{\sum_i d(i)}{N \cdot \sum_j L(j)} \\ \overline{t}_j &= \frac{\sum_k t(j_k)}{N(j) \cdot L(j)}, \overline{d}_j = \frac{\sum_k d(j_k)}{N(j) \cdot L(j)}. \end{aligned} \tag{6}$$

5.2. Experimental Result. The optimized AI video analysis model is applied on CCTV videos to extract the real-time traffic data for the study site. The performance of the AI model optimization is summarized in Table 5. First, the model is significantly compressed of which size is decreased by 97.8% compared to the original model. This means that the compressed model takes only 2.2 Mb if the original takes 100 Mb because a number of weight parameters are eliminated. Second, the optimized model can process incoming video data in near real time. In general, inference speed measures the performance of AI model lightweighting, and 30 FPS is considered as "real-time." On the installed edge device, the proposed model shows 29.49 FPS which is near real time. Finally, the model maintains a similar level of accuracy despite the compression. In general, accuracy tends to decrease when the parameters are eliminated through model compression. However, the size of the model can be reduced to a level that maintains the accuracy by selectively eliminating less-contributing parameters. To test accuracy, the model is trained using 8,824 collected image frames including cars, buses, trucks, motorcycles, and pedestrians. Then, the model is validated with 100 unseen image frames of which ground truth is manually counted.

Next, we utilize the real-time traffic data extracted from the smart intersections as input variables in equations (1)–(4) to calculate the optimal offset for each intersection. We apply mixed-integer nonlinear programming (MINLP)

Table 5: Performance of edge AI video analysis model.

Metrics	Measurement	Results
Efficiency of model compression	(1 − (compressed model size/previous model size)) × 100	97.8%
Inference speed	Processible number of frames in a second (frame per second, FPS)	29.49 FPS
Accuracy in object detection	(correctly classified number/total number of objects) × 100	93.64%

to solve the optimization problem in equation (1) that involves integer variables using CPLEX (version 12.3) API provided by IBM. The calculated optimal solutions are then applied as the offset value of each intersection into the AIMSUN environment.

For a detailed evaluation, we analyze the MoEs not only for the entire network but also for the selected 5 specific routes, as illustrated in Figure 4. The first route, named by Path 1, corresponds to the major traveling direction on the mainstream which has the highest level of traffic volume. On the other hand, Path 2 is selected by the opposite direction on the mainstream to evaluate the effect of maximizing bidirectional bandwidth. Moreover, we also consider Path 3 and Path 4 which have relatively high traffic demands among the minor streams to measure the coordination effects on the side-street left-turning flows. In addition, Path 5 is also included of which signal is coordinated to the mainstream despite the traffic demand is significantly low.

The numerical results are summarized in Figure 7. Most of all, it is found that LT2 improves network efficiencies in every MoE. Compared to the existing TOD, the average number of stops is decreased from 1.04 to 0.96, indicating approximately 7.69% improvement. Similarly, the average delay and travel time are improved by approximately 6.2% and 2.92%, respectively. PASSER2 and MULTIBAND also improve the network performances compared to TOD.

However, upon examining the results for individual paths, it becomes evident that LT2 shows better performances. Specifically, both MULTIBAND and LT2 similarly exhibit the improvement on the mainstream, Path 1, while PASSER2 shows the worst performance. On the other hand, for the two major side-street left-turning flows, Path 3 and Path 4, it is remarkable that LT2 improves the performance than MULTIBAND. It implies that the LT2 reduces unnecessary delays of the side-streets with relatively high demands. Additionally, it can be seen that the existing TOD unnecessarily yields the most effective signal coordination to Path 5 which has the lowest demand.

The changes of bandwidth can be observed in Figure 8, and it corresponds with the numerical results analyzed in Figure 7. In the outbound direction, the LT2 and MULTIBAND models present an expanded bandwidth ⓐ for the major flow, surpassing the TOD and PASSER2 models. Therefore, they allow a larger number of vehicles to pass through the corridor (Path 1) without stopping. In addition, the left-turning flows for Paths 3, 4, and 5 are allocated to ⓑ, ⓒ, and ⓔ, respectively. It is observed that TOD inefficiently assigns wider bandwidth to ⓔ, yet relatively narrower bandwidth to ⓑ. In contrast, the LT2 model effectively distributes sufficient bandwidths ⓑ and ⓒ to Paths 3 and 4, which have relatively high demands, and manages to efficiently accommodate Path 5 as well, unlike the MULTIBAND, which fails to secure bandwidth ⓔ.

6. Discussion

In this study, each of the four signal coordination models requires distinct spatial and temporal resolution for traffic data. The existing TOD, based on AADT statistics with low temporal resolution, shows significant limitations in adapting to fluctuating traffic demands. To improve this, real-time traffic flow data collected by loop detectors installed in straight lanes of the mainstream conventionally facilitate the signal coordination algorithms, such as PASSER2 and MULTIBAND. These conventional signal coordination algorithms improve the network efficiency centered at the mainstream, as shown in Figure 7. However, there still have been signal coordination failures on irregular travel demands during nonpeak hours occurring unnecessary delays of the side-streets with relatively high demands (e.g., degradation of MULTIBAND for Paths 3 and 4).

The state-of-the-art signal coordination methods, including LT2, propose novel methods to coordinate the multidirectional traffic flows in order to mitigate the congestion on the side-streets with relatively high demands. Although these algorithms demonstrate significant improvement in their simulation-based experiments, they would encounter some challenges with regard to the practical implementation. These methods require high-resolution real-time traffic data for the turning traffic flows of each intersection, such as turning ratios and queueing vehicle numbers, in order to calculate the accurate values for the signal timings.

In this aspect, the edge AI-based smart intersection proposed in this study highlights the potential use of these novel signal coordination methods by serving high-resolution traffic data in real time. Taking the advantages of using CCTVs and AI, the edge AI-based smart intersection provides abundant traffic data of point/section-based information, and even contextualized information, unlike the other traditional VDS. Accordingly, this study provides an application of improving signal coordination using real-time traffic data collected from edge AI-based smart intersections. By leveraging these data, the experimental results indicate that LT2 alleviates the coordination failure problem for nonpeak hour demands in the study site.

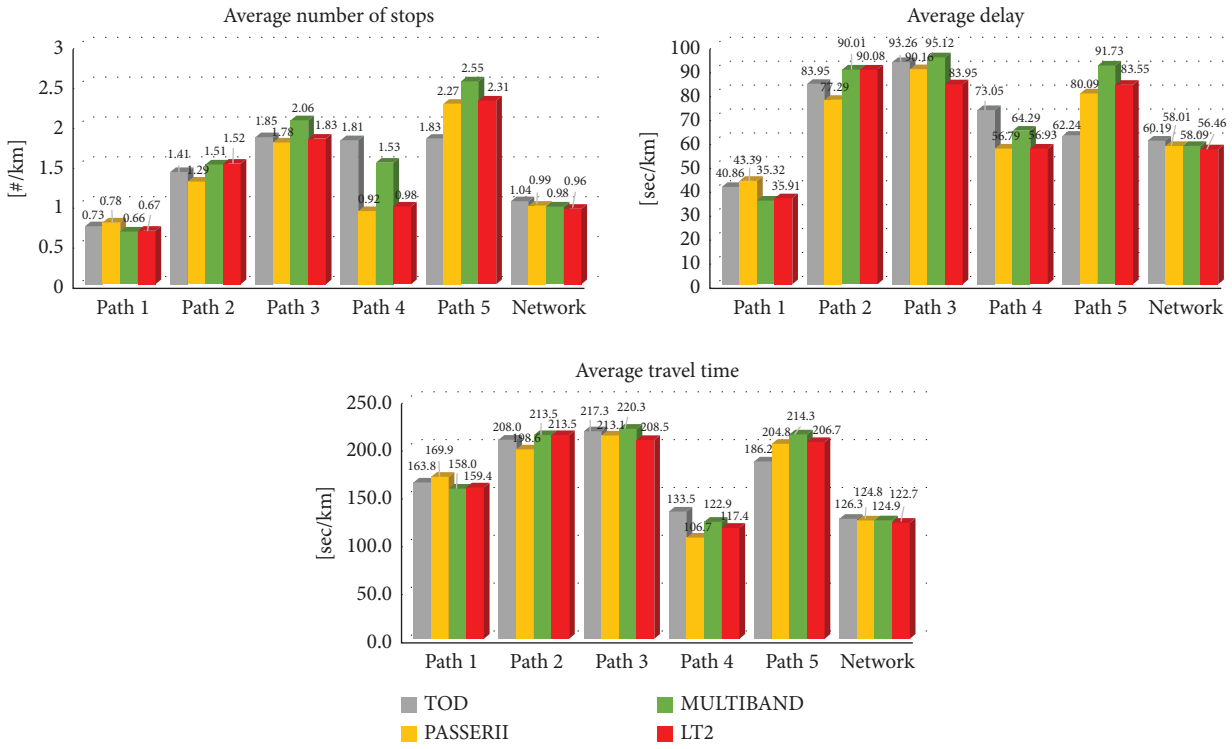

Figure 7: Experimental results.

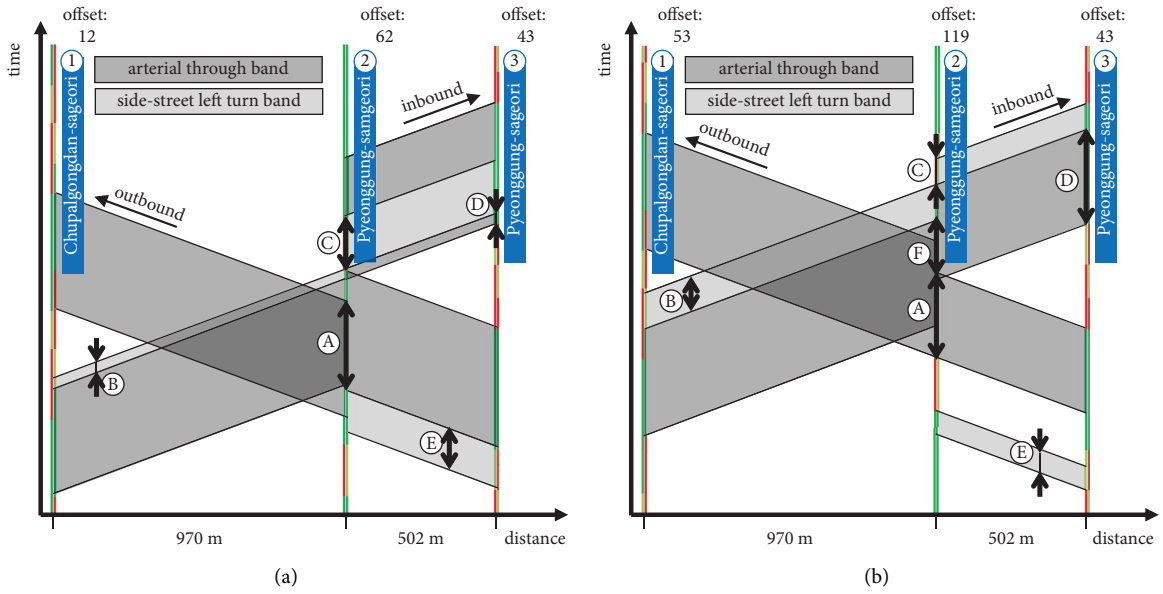

Figure 8: Continued.

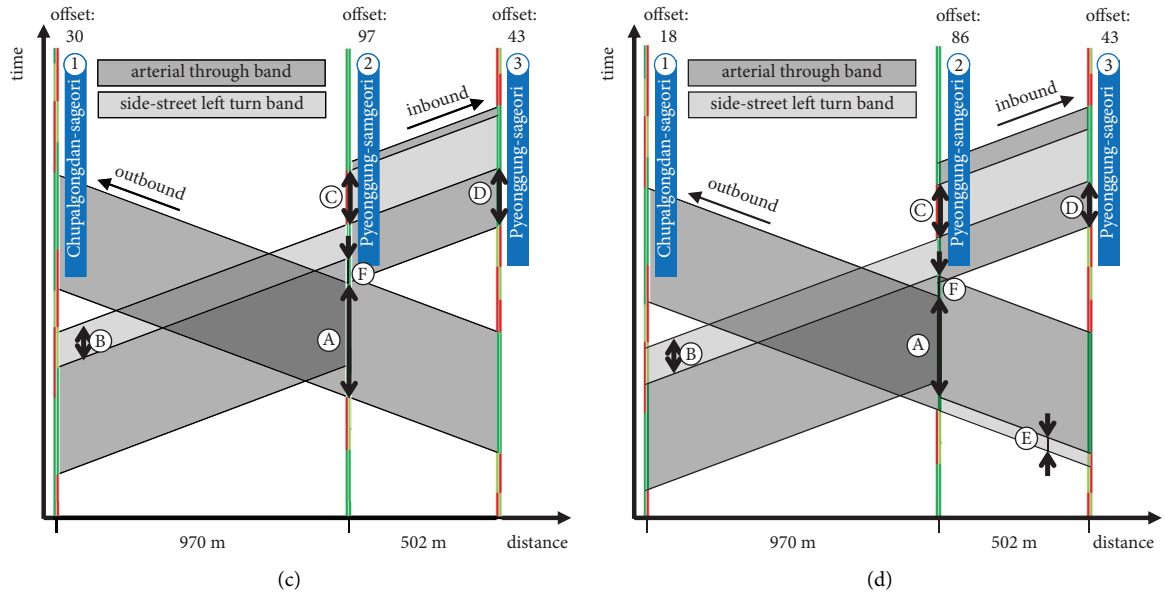

Figure 8: Visualization of bandwidth in time-space diagram. (a) TOD. (b) PASSER2. (c) MULTIBAND. (d) LT2.

7. Conclusion

The goal of this study is to construct edge AI-based smart intersections utilizing AI optimization techniques and to provide their application for traffic signal coordination. To this end, we install smart intersections on three consecutive intersections of Route 45 in Pyeongtaek city, South Korea, and collect the real-time traffic data by applying the edge AI video analysis model. The model compressed and optimized via NetsPresso maintains a similar level of accuracy (93.64%), even if the size is reduced by 97.8% compared to the original. Next, we utilize a LT2 model to treat the coordination failure problem in nonpeak hours occurring unnecessary delays of the side-streets with relatively high demands. We complement some constraint conditions in order to consider the compatibility with the current legacy signal control system. The experiment is conducted on the virtual environment of which geometry and traffic demand are configured based on the features of the installed smart intersections. The numerical results conclude that the calculated optimal offsets calculated by the LT2 model effectively manage bandwidths for multidirectional flows based on the real-time traffic demands collected from the edge AI-based smart intersections.

The main contribution of this research is that it introduces an edge AI-based smart intersection. Although smart intersections have been prevalent in many cities, there are a few drawbacks in their operations. In this regard, this study demonstrates the effectiveness of edge AI-based smart intersections by extracting real-time traffic data from CCTV video data, even on low-powered edge devices, with high accuracy. Furthermore, this study explores the application of edge AI-based smart intersections to a practical signal coordination problem using a state-of-the-art algorithm that requires high-resolution real-time traffic data for all turning traffic flows of each intersection.

This research serves as a preliminary study to validate the effectiveness of edge AI-based smart intersections in signal coordination before conducting on-site tests. The primary future plan is to carry out experiments on actual roads rather than in a simulated environment. Subsequently, the performance of the proposed method will be assessed using real traffic data. Furthermore, we plan to explore additional signal control variables, including green splits or cycle time, as part of our effort to revise the legacy system. Moreover, future studies will involve the development of an enhanced model, leveraging a broad spectrum of traffic data obtained from edge AI-based smart intersections.

Data Availability

The captured traffic video data of this study are available from the corresponding author upon request.

Disclosure

Current affiliation was under Jinwon Yoon, a Post-doctoral research fellow. Korea Advanced Institute of Science and Technology (KAIST), Mechanical Engineering Research Institute, 193 Munji-ro, Yuseong-gu, Daejeon 34051, Republic of Korea.

Conflicts of Interest

The authors declare that they do not have any conflicts of interest regarding the publication of this paper.

References

[1] A. G. Sims and K. W. Dobinson, "The sydney coordinated adaptive traffic (SCAT) system philosophy and benefits," *IEEE Transactions on Vehicular Technology*, vol. 29, no. 2, pp. 130–137, 1980.

[2] P. B. Hunt, D. I. Robertson, R. D. Bretherton, and M. C. R. Hunt, "The SCOOT on-line traffic signal optimisation technique," *Traffic Engineering and Control*, vol. 23, no. 4, p. 1982, 1982.

[3] N. H. Gartner, "OPAC: a demand-responsive strategy for traffic signal control," *Transportation Research Record*, vol. 906, pp. 75–81, 1983.

[4] A. C. Egea, S. Howell, M. Knutins, and C. Connaughton, "Assessment of reward functions for reinforcement learning traffic signal control under real-world limitations," in *Proceedings of the 2020 IEEE International Conference on Systems, Man, and Cybernetics (SMC)*, Toronto, ON, Canada, October 2020.

[5] Yunex Traffic, "Traffic detectors [product broucher]," 2023, https://www.yunextraffic.com/portfolio/smart-intersection/traffic-detectors/.

[6] Swarco, "SMART green intelligent solutions for smart cities [product broucher]," 2023, https://www.swarco.com/products/software/urban-traffic-management/smart-intersection.

[7] X. Liang, X. Du, G. Wang, and Z. Han, "A deep reinforcement learning network for traffic light cycle control," *IEEE Transactions on Vehicular Technology*, vol. 68, no. 2, pp. 1243–1253, 2019.

[8] T. Chu, J. Wang, L. Codeca, and Z. Li, "Multi-agent deep reinforcement learning for large-scale traffic signal control," *IEEE Transactions on Intelligent Transportation Systems*, vol. 21, no. 3, pp. 1086–1095, 2020.

[9] J. Yoon, K. Ahn, J. Park, and H. Yeo, "Transferable traffic signal control: reinforcement learning with graph centric state representation," *Transportation Research Part C: Emerging Technologies*, vol. 130, Article ID 103321, 2021.

[10] A. Krizhevsky, I. Sutskever, and G. E. Hinton, "Imagenet classification with deep convolutional neural networks," *Advances in neural information processing systems*, vol. 25, 2012.

[11] R. Girshick, J. Donahue, T. Darrell, and J. Malik, "Rich feature hierarchies for accurate object detection and semantic segmentation," in *Proceedings of the IEEE conference on computer vision and pattern recognition*, New York, NY, USA, June 2014.

[12] R. Girshick, "Fast R-CNN," in *Proceedings of the IEEE international conference on computer vision*, Canada, July 2015.

[13] S. Ren, K. He, R. Girshick, and J. Sun, "Faster r-cnn: towards real-time object detection with region proposal networks," *Advances in neural information processing systems*, vol. 28, 2015.

[14] J. Redmon, S. Divvala, R. Girshick, and A. Farhadi, "You only look once: unified, real-time object detection," in *Proceedings of the IEEE conference on computer vision and pattern recognition*, New York, NY, USA, June 2016.

[15] W. Liu, D. Anguelov, D. Erhan et al., "SSD: single shot multibox detector," in *Computer Vision--ECCV 2016*, B. Leibe, J. Matas, N. Sebe, and M. Welling, Eds., pp. 21–37, Springer, Amsterdam, The Netherlands, 2016.

[16] J. D. C. Little, M. D. Kelson, and N. H. Gartner, *MAXBAND: A Versatile Program for Setting Signals on Arteries and Triangular Networks*, Alfred P. Sloan School of Management, Massachusetts Institute of Technology, Cambridge, MA, USA, 1981.

[17] N. H. Gartner, S. F. Assman, F. Lasaga, and D. L. Hou, "A multi-band approach to arterial traffic signal optimization," *Transportation Research Part B: Methodological*, vol. 25, no. 1, pp. 55–74, 1991.

[18] C. Zhang, Y. Xie, N. H. Gartner, C. Stamatiadis, and T. Arsava, "AM-band: an asymmetrical multi-band model for arterial traffic signal coordination," *Transportation Research Part C: Emerging Technologies*, vol. 58, pp. 515–531, 2015.

[19] C. Chen, X. Che, W. Huang, and K. Li, "A two-way progression model for arterial signal coordination considering side-street turning traffic," *Transportation Business: Transport Dynamics*, vol. 7, no. 1, pp. 1627–1650, 2019.

[20] Z. Ge, S. Liu, F. Wang, Z. Li, and J. Sun, "YOLOX: exceeding YOLO series in 2021," *arXiv preprint*, vol. 2107, 2021.

[21] H. Li, A. Kadav, I. Durdanovic, H. Samet, and H. P. Graf, "Pruning Filters for Efficient ConvNets," *arXiv preprint*, 2016, http://arxiv.org/abs/1608.08710.

[22] D. S. Bolme, J. R. Beveridge, B. A. Draper, and Y. M. Lui, "Visual object tracking using adaptive correlation filters," in *Proceedings of the 2010 IEEE Computer Society Conference on Computer Vision and Pattern Recognition*, San Francisco, CA, USA, June 2010.